The α-helical FXXΦΦ motif in p53: TAF interaction and discrimination by MDM2

Motonari Uesugi* and Gregory L. Verdine†

Department of Chemistry and Chemical Biology, Harvard University, Cambridge, MA 02138

Edited by Robert Tjian, University of California, Berkeley, CA, and approved October 12, 1999 (received for review June 1, 1999)

Transcriptional activation domains share little sequence homology and generally lack folded structures in the absence of their targets, aspects that have rendered activation domains difficult to characterize. Here, a combination of biochemical and nuclear magnetic resonance experiments demonstrates that the activation domain of the tumor suppressor p53 has an FXXΦΦ motif (F, Phe; X, any amino acids; Φ, hydrophobic residues) that folds into an α-helix upon binding to one of its targets, hTAF$_{II}$31 (a human TFIID TATA box-binding protein-associated factor). MDM2, the cellular attenuator of p53, discriminates the FXXΦΦ motif of p53 from those of NF-κB p65 and VP16 and specifically inhibits p53 activity. Our studies support the notion that the FXXΦΦ sequence is a general α-helical recognition motif for hTAF$_{II}$31 and provide insights into the mechanistic basis for regulation of p53 function.

The tumor suppressor p53 plays a pivotal role in maintaining the genomic integrity of the cell by arresting cell growth or initiating apoptosis (1). One mechanism by which the p53 protein exerts its antiproliferative activity is by inducing the transcription of genes that control cell growth. The ability of p53 to function as a transcription factor depends critically on its two modular domains: an NH_2-terminal transcriptional activation domain (amino acids 1–42) and a central DNA-binding domain (amino acids 120–290). The DNA-binding domain provides gene specificity by binding to specific DNA sequences, and the activation domain stimulates transcription by interacting with hTAF$_{II}$31 and hTAF$_{II}$70 (2, 3) in addition to cellular coactivators p300/CBP (4–7). Although mutations in p53 that arise in human cancers cluster in the DNA-binding domain, functional deregulation of the activation domain also is associated with human tumorigenesis (8). The oncoprotein MDM2, a cellular attenuator of p53 that is overexpressed in certain tumors (9), and the adenovirus E1B 55-kDa oncoprotein (10) are known to down-regulate the p53 protein by masking its activation domain (11) and accelerating its destruction by the ubiquitin–proteosome pathway (12, 13). The activation domain also plays a central role in responding to cellular signals upon DNA damage. The ATM protein, which is encoded by the gene responsible for the human genetic disorder ataxia telangiectasia (14, 15), and the DNA-activated protein kinase (16, 17) have been shown to up-regulate the p53 protein upon DNA damage by phosphorylating the activation domain of p53. Therefore, the p53 activation domain acts as a relay switch to control the activation of the p53 protein in response to the status of the cellular genome.

The preponderance of acidic amino acid residues in the p53 activation domain suggests that it is a member of the "acidic" class of activators. We previously demonstrated that the VP16 activation domain, a prototypical acidic activator, undergoes an induced transition from random coil to α-helix upon binding to hTAF$_{II}$31, with residues along one face of the nascent helix making intermolecular contacts to hTAF$_{II}$31 (18). Identification of these contacting residues suggested that FXXΦΦ (F, Phe; X, any amino acids; Φ, hydrophobic residues) might represent a general recognition motif in acidic activation domains for hTAF$_{II}$31. Here we extend our analysis of the FXXΦΦ motif to the p53 activation domain. A combination of biochemical and NMR experiments provides further evidence that the p53 activation domain has a functional FXXΦΦ motif that folds up into a short α-helix upon binding to hTAF$_{II}$31. It is also shown that the MDM2 protein discriminates among FXXΦΦ motifs in acidic activators, thus providing a mechanism for the specific inhibition of p53. Comparison between the results on the TAF$_{II}$31 interaction motif and the earlier x-ray crystal structure of the p53 activation domain bound to MDM2 (11) allowed identification of Trp^{23} and Leu^{26} as the primary elements in p53 that enable MDM2 to discriminate the hTAF$_{II}$31-binding site in p53 against those in VP16 and p65. This study not only supports the notion that the FXXΦΦ sequence is a general α-helical recognition motif for hTAF$_{II}$31 but also provides insight into the cellular mechanisms controlling transcriptional activation by p53.

Materials and Methods

Proteins. TAF$_{1–140}$, glutathione *S*-transferase (GST) fusion proteins, and GAL4$_{1–94}$ fusions were expressed and purified as described (18). The expression plasmid for MDM2$_{3–109}$ was constructed by cloning a coding DNA fragment generated with PCR into the *Escherichia coli* vector pLM1. Transformed cells were grown at 37°C to an OD_{600} of 0.2 and then at 30°C to an OD_{600} of 0.5 in 1 liter of medium. The culture then was induced with 0.4 mM isopropyl β-D-thiogalactopyranoside and harvested 5 hr later. The French-pressed bacterial mixture (10 mM Tris·HCl, pH 7.4/400 mM NaCl/0.1 mM PMSF) was centrifuged at 30,000 × *g* for 20 min. To the supernatant (10 ml) was added 0.5 ml of 5% polyethyleneimine. After swirling on ice, the sample was centrifuged at 30,000 × *g* for 20 min. The proteins in the supernatant were precipitated with ammonium sulfate. MDM2$_{3–109}$ was purified by using SP Sepharose and Q Sepharose columns (Pharmacia) and characterized by electrospray ionization mass spectroscopy.

Protein–Protein Interaction Assays. GST fusion beads (loaded with 200 μg of protein) were incubated with 50 μg of TAF$_{1–140}$ in 200 μl of binding buffer (20 mM Tris·HCl, pH 7.4/50 mM NaCl/2 mM DTT/10 mM $MgCl_2$/0.01% Nonidet P-40/10% glycerol] at 4°C for 1 hr and then washed three times with 200 μl of the same buffer. The samples were dissolved in SDS/PAGE loading buffer and analyzed by SDS/PAGE. For the interaction with MDM2$_{3–109}$, 3.8 μg of MDM2$_{3–109}$ was used for each binding.

NMR Studies. p53$_{9–25}$ was synthesized on an automated synthesizer (rink resin), purified by HPLC, and characterized by NMR and electrospray ionization mass spectroscopy. The peptide was dissolved in 95% H_2O plus 5% ^2H_2O containing 150 mM KCl,

This paper was submitted directly (Track II) to the PNAS office.

Abbreviations: GST, glutathione *S*-transferase; NOE(SY), nuclear Overhauser effect (spectroscopy); CBP, CREB binding protein.

*Present address: Department of Biochemistry, Baylor College of Medicine, Houston, TX 77030.

†To whom reprint requests should be addressed. E-mail: verdine@chemistry.harvard.edu.

The publication costs of this article were defrayed in part by page charge payment. This article must therefore be hereby marked "*advertisement*" in accordance with 18 U.S.C. §1734 solely to indicate this fact.

5 mM perdeuterated DTT, 20 mM perdeuterated Tris-AcOH (pH 6.2), and 10 μM EDTA, and then the pH of the solution was adjusted to $\approx$6.0 by adding dilute KOH. The final concentration of $p53_{9-25}$ was determined by UV absorption to be 2.8 mM. NMR experiments were performed in the absence or presence of TAF_{1-140} (300 μM) on a Bruker DMX500 spectrometer (Bruker, Billerica, MA) equipped with a *z*-shielded gradient triple resonance probe. The sequential assignment of the peptide signals was obtained by using a combination of total correlation spectroscopy (TOCSY), double quantum-filtered correlated spectroscopy (DQF-COSY), and nuclear Overhauser effect spectroscopy (NOESY) data sets of a free peptide sample. Sequential $d_{\alpha N}(i, i+1)$ NOEs were, although weak, observed in the NOESY spectra of the free peptide, which served as a basis for the complete sequential assignment. In the NOESY spectra, 512 free induction decays were recorded at 300 K with mixing times of 200 and 350 ms. The data were processed with the FELIX software (Biosym Technologies, San Diego) with appropriate apodization and zero-filling. We observed large transferred effects as demonstrated by numerous additional NOE cross-peaks in the presence of TAF_{1-140}. This is in good agreement with the relatively weak (fast-exchanging) interaction between the two proteins as revealed by GST pull-down experiments.

Transcription Assays. *In vitro* transcription assays were performed as described (18). For the analysis of *in vivo* transcription, Jurkat cells ($\approx 2 \times 10^6$ cells) were transfected (10 μM DMRIE-C; GIBCO/BRL) with reporter plasmid pG5IL2SX (2 μg) and an expression plasmid of activators (1 μg). After 20-hr incubation, aliquots were assayed for secreted alkaline phosphatase activity as described (19). Cells were harvested and analyzed for DNA binding in gel mobility-shift assays by using a *Bam*HI-*Hin*dIII fragment of pG_5E4 (20). Similar amounts of DNA–protein complexes were observed in autoradiograms, showing that mutant proteins were expressed to comparable levels. In MDM2 coexpression experiments, 2 μg of pG5IL2SX, 0.5 μg of each activator expression plasmid, and 0.5–2 μg of MDM2 expression plasmid pCHDM1B were used.

Results

FXXΦΦ Motifs in p53 and NFκB p65. The acidic activation domains of p53 and NFκB p65, which have been reported to interact with $hTAF_{II}31$ (2, 3, 21), contain FXXΦΦ motifs. Apart from this, there is little sequence similarity between p53, p65, and VP16 activation domains (Fig. 1*A*) (18). To evaluate the FXXΦΦ sequences in p53 and p65, two short peptides from the activation domains of p53 and p65 that encompass the FXXΦΦ sequences ($p53_{9-25}$ and $p65_{532-548}$) were analyzed for the ability to bind $hTAF_{II}31$ and to activate transcription. To assay for $hTAF_{II}31$-binding activity, each peptide was fused to GST and analyzed for the ability to pull down the NH_2-terminal 140-aa fragment of $hTAF_{II}31$ (TAF_{1-140}), this domain being sufficient for activator binding (18). As shown in Fig. 1*B*, both $p53_{9-25}$ and $p65_{532-548}$ exhibited significant binding activity for TAF_{1-140}. $p53_{9-25}$ and $p65_{532-548}$ then were fused to the GAL4 DNA-binding domain, and the resulting proteins were analyzed for the ability to activate transcription *in vitro* with HeLa nuclear extracts. $p53_{9-25}$ and $p65_{532-548}$ activated transcription of the reporter construct containing five GAL4 recognition sites to the same extent as the minimal activation peptide from VP16 (Fig. 1*C*). It is noteworthy that the full-length p53 activation domain stimulated transcription more strongly than $p53_{9-25}$, suggesting the presence of other activation elements in $p53_{1-52}$ that internally synergize with $p53_{9-25}$. Nonetheless, mutational studies on p53 have shown that Phe^{19}, Leu^{22}, and Trp^{23} are critical for transcriptional activation by $p53_{1-52}$, consistent with the notion that the FXXΦΦ motif represents the core segment of the activation domain (24, 25).

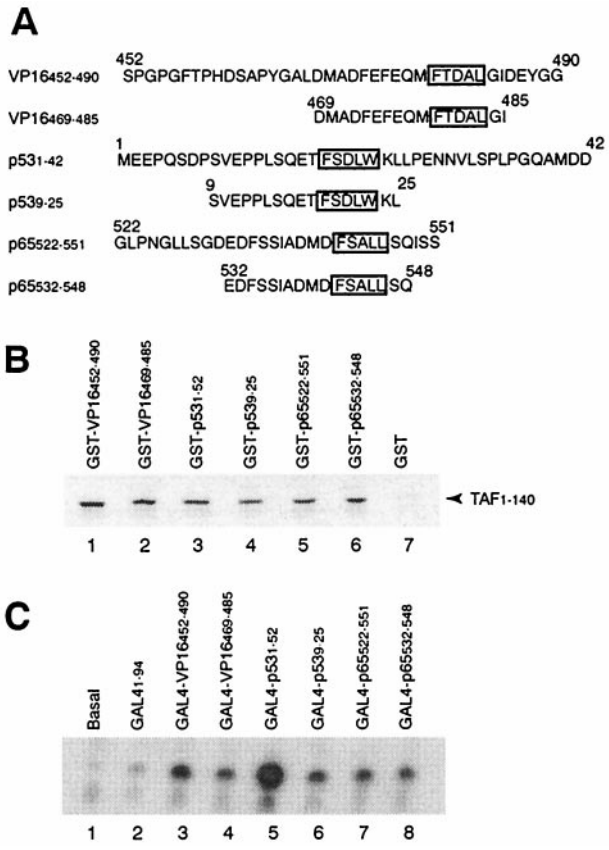

Fig. 1. The activation domains of p53 and NF-κB p65 contain a FXXΦΦ motif. (*A*) Amino acid sequences of the activation domains of VP16, p53, and p65. FXXΦΦ sequences are indicated by boxes. (*B*) *In vitro* protein–protein interaction assays. Binding of TAF_{1-140} to GST-$VP16_{452-490}$ (lane 1), GST-$VP16_{469-485}$ (lane 2), GST-$p53_{1-52}$ (lane 3), GST-$p53_{9-25}$ (lane 4), GST-$p65_{522-551}$ (lane 5), and GST-$p65_{532-548}$ (lane 6) is evident. TAF_{1-140} is not retained on GST resin (lane 7). The position of TAF_{1-140} is indicated by an arrowhead. (*C*) *In vitro* transcription assays. Transcriptional activation by activation domains fused with the GAL4 DNA-binding domain was assayed in HeLa nuclear extracts. The reactions contained 2 pmol of the purified proteins and 100 ng of pG5BCAT template containing the adenovirus E1b promoter linked to five GAL4 recognition sites. The products of the transcription reactions were analyzed by primer extension. Lane 1 shows basal transcription without GAL4 proteins. The transcriptional activation by GAL4-$VP16_{452-490}$ (lane 3), GAL4-$VP16_{469-485}$ (lane 4), GAL4-$p53_{1-52}$ (lane 5), GAL4-$p53_{9-25}$ (lane 6), GAL4-$p65_{522-551}$ (lane 7), and GAL4-$p65_{532-548}$ (lane 8) is greater than that observed for GAL4 alone (lane 2).

These results raised the possibility that FXXΦΦ comprises a core activation motif in all three of these activation domains.

The FXXΦΦ Motif in p53 Folds Up into an α-Helix upon Binding to $hTAF_{II}31$. To determine the conformation of $p53_{9-25}$ when bound to TAF_{1-140}, we performed transferred NOE (TRNOE) NMR experiments. TRNOE relies on rapid exchange between free and bound states of a small ligand interacting weakly with its macromolecular receptor (22). Under conditions of rapid exchange, negative NOEs conveying conformational information of the bound ligand can be transferred to the resonances of the free ligand. NOEs from the free ligand itself approach zero because of its low molecular weight. Therefore, when the molecular weight of a ligand is low enough, it is possible to detect NOEs primarily from the bound ligand in the presence of substoichemetric amounts of the receptor. Indeed, free $p53_{9-25}$ exhibited few NOEs, as expected for a low-molecular-weight peptide tumbling freely in solution. Although the presence of several weak NOEs between amide protons suggested transient

formation of some secondary structure within the FXXΦΦ sequence of $p53_{9-25}$ (23), the overall lack of strong interresidue NOEs indicated the absence of a stably folded structure. Furthermore, the circular dichroism spectrum of the peptide at 27°C exhibited features characteristic of random coil structure (not shown). In the presence of TAF_{1-140}, however, numerous additional NOE cross-peaks appeared, indicative of a large, transferred NOE effect. The appearance of NOE cross-peaks between successive amide protons in the main chain (Fig. 2*A*) suggests the formation of an α-helix. However, some of the interresidue NOEs in the $\alpha\beta$(i, i+3) region were difficult to interpret, owing to signal overlap. To circumvent this problem, a shorter peptide, $p53_{10-25}$, was used for further NMR studies. Its lower molecular weight and fewer signals allowed us to establish the presence of strong $\alpha\beta$(i, i+3) NOE connectivities in the bound state; these are most characteristic of an α-helical structure (Fig. 2*B*). The overall pattern of NOEs summarized in Fig. 2*C* indeed indicates formation of an α-helix in the region from Thr^{18} to Lys^{24} when bound to TAF_{1-140}. The α proton of Leu^{22} has an NOE with a methyl group of Leu^{25} rather than its β protons, suggesting, perhaps, a slight deviation from a canonical α-helix structure at Leu^{25}. As shown in Fig. 2*C*, the α-helix induced in p53 by binding to TAF_{1-140} is shorter than that induced in VP16; the p53 helix has only two turns but still encompasses the FXXΦΦ motif, FSDLW. We conclude that an FXXΦΦ sequence in the p53 activation domain is a core recognition element for $hTAF_{II}31$ that folds up into a short α-helix upon binding.

Extensive mutational studies on p53 have identified Phe^{19}, Leu^{22}, and Trp^{23} as critical residues for transcriptional activation by p53 (24, 25). The projection of residues 18–24 of the p53 activation domain onto a helical wheel reveals that these three residues lie along one face of the helix (Fig. 3*A*). Substitution of Phe^{19} and Trp^{23} with Ala greatly decreased $hTAF_{II}31$ binding (Fig. 3*B*) and transcriptional activation in transiently transfected cells (Fig. 3*C*), despite the fact that these substitutions stabilize α-helical structure. Thus, it seems likely that these three residues make direct contacts with chemically complementary residues of $hTAF_{II}31$.

Helix Disruption Impairs TAF Binding and Transcriptional Activation. The significance of α-helix formation for transcriptional activation by p53 was examined through the effects of helix disruption on interaction with TAF_{1-140} *in vitro* and transcriptional activation *in vivo*. To disrupt the α-helix formation, Asp^{21} at the third position of the FXXΦΦ motif in the p53 activation domain was substituted with helix-breaking Pro. Asp^{21} was deemed suitable for the analysis because a helical wheel suggested that Asp^{21} is located on the other side of the helix from the interface with $hTAF_{II}31$ and because substitution of Asp^{21} with Ala had no significant effect on TAF binding and transcriptional activation (Fig. 4). In contrast, substitution with Pro greatly impaired TAF binding and abolished transcriptional activation in transfected cells (Fig. 4). The mutant proteins were expressed in transfected cells at equal levels as demonstrated by gel mobility-shift analyses (Fig. 4*B*). Therefore, the loss of function in the Asp^{21}-to-Pro mutant can be considered because of disruption of the helical structure that is required for the FXXΦΦ motif of p53 to interact with $hTAF_{II}31$.

MDM2 Discriminates Among FXXΦΦ Motifs. The short α-helix that is induced upon binding to TAF_{1-140} is almost identical to the one revealed in the crystal structure of $p53_{15-29}$ bound to MDM2 (11). This observation indicates that the interaction between p53 and MDM2 parallels that between p53 and $hTAF_{II}31$ and supports the notion that MDM2 inhibits the p53 function by tightly masking the FXXΦΦ sequence in the p53 activation domain. Because the activation domains of p65 and VP16 share

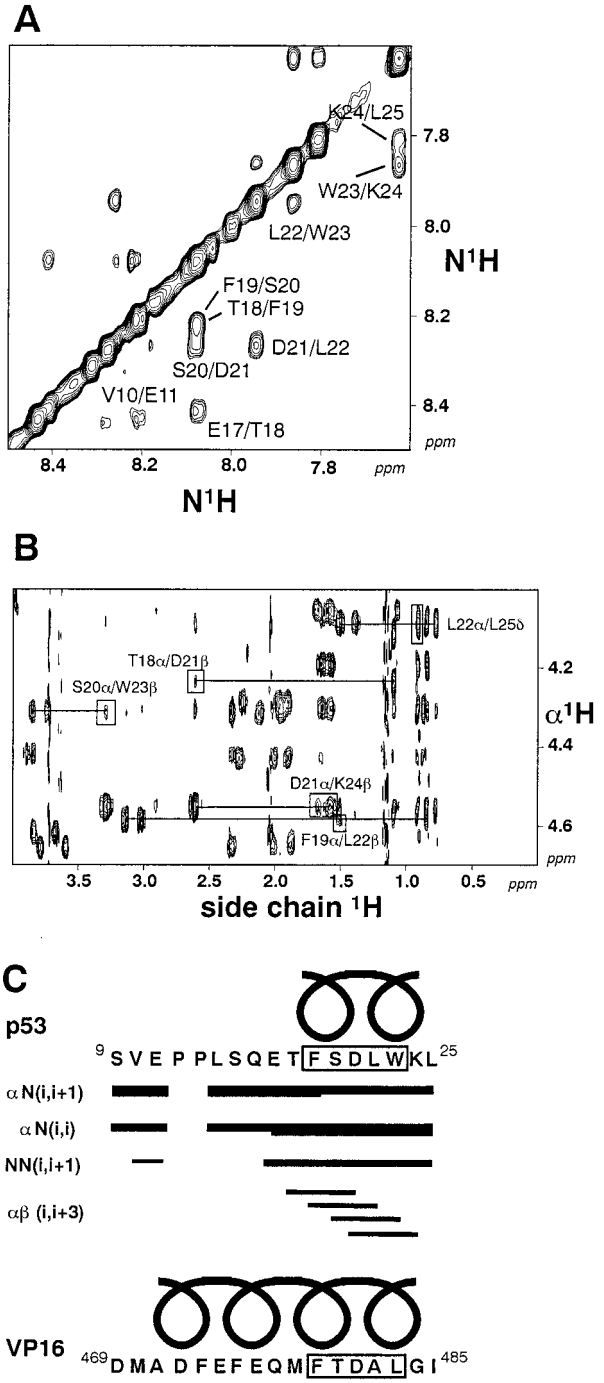

Fig. 2. Transferred NOE (TRNOE) experiments. (*A*) The amide region of a 200-ms NOESY spectrum of $p53_{9-25}$ (2.8 mM) in the presence of TAF_{1-140} (0.3 mM). The identities of residues that exhibit NOE cross-peaks in this region are indicated. (*B*) The $\alpha\beta$ region of a 350-ms NOESY spectrum of $p53_{10-25}$ (3.5 mM) in the presence of TAF_{1-140} (0.3 mM). The identities of key NOEs are indicated. (*C*) Summary of the NOEs observed from the TRNOE experiments of $p53_{9-25}$ and $p53_{10-25}$ and comparison between $p53_{9-25}$ and $VP16_{469-485}$. The thickness of the lines indicates the relative intensities of the NOE cross-peaks. Black coils above the sequences represent the regions over which α-helix induction is observed upon binding to TAF_{1-140}. The data of $VP16_{469-485}$ are from ref. 18.

FXXΦΦ sequences that appear to interact with $hTAF_{II}31$, we were interested in testing whether MDM2 has affinity for these activators as well. As shown in Fig. 5*A*, $MDM2_{3-109}$ binds only the p53 activation domain. Thus, MDM2 discriminates the $hTAF_{II}31$ binding motif of p53 from those of VP16 and p65.

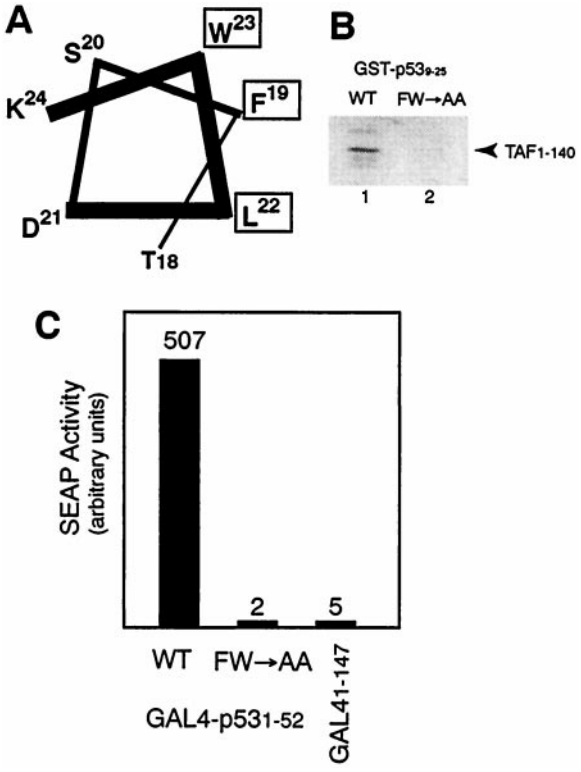

Fig. 3. (*A*) Helical wheel presentation of residues 18–24 of p53. The residues that mutational studies have shown to be critical for transcriptional activation are indicated by boxes. (*B*) Substitution of Phe^{19} and Trp^{23} with Ala in $p53_{9-25}$ significantly reduces binding to TAF_{1-140} *in vitro*. It is evident that binding of GST-$p53_{9-25}$ ($F^{19}W^{23} \rightarrow$ AA mutant) to TAF_{1-140} (lane 2) is much weaker than that of GST-$p53_{9-25}$ [wild type (WT); lane 1]. (*C*) Transient transfection assays. Expression plasmids encoding GAL4-$p53_{1-52}$ and its mutant were transiently transfected into Jurkat cells together with a reporter plasmid in which the production of secreted alkaline phosphatase (SEAP) is under control of an IL-2 promoter carrying five GAL4-binding sites.

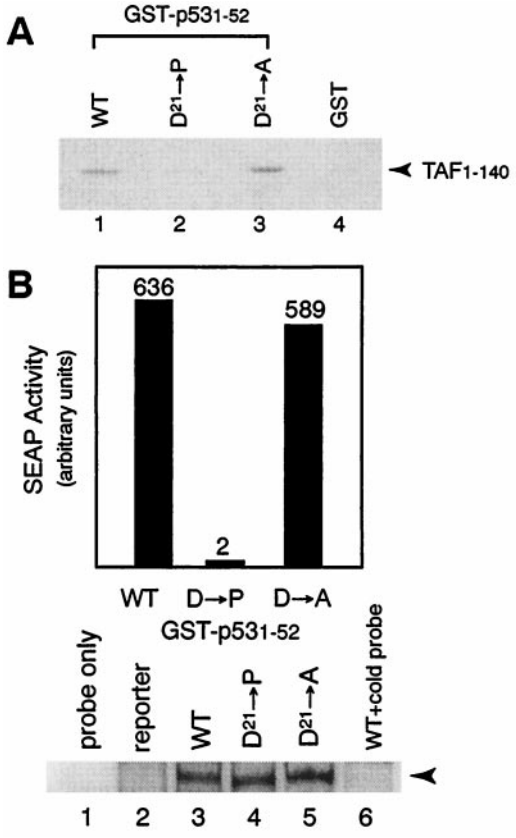

Fig. 4. Helix disruption greatly impairs TAF binding and transcriptional activation. (*A*) *In vitro* protein–protein interaction assays. Asp^{21} at the third position of the FXXΦΦ motif in the p53 activation domain was substituted with helix-breaking Pro. This substitution greatly reduced the binding affinity for TAF_{1-140} (compare lanes 1 and 2), whereas substitution of Asp^{21} with Ala had no significant effect on TAF binding (lane 3). TAF_{1-140} is not retained on GST resin (lane 4). The position of TAF_{1-140} is indicated by an arrowhead. (*B*) Transient transfection assays. Expression plasmids encoding GAL4-$p53_{1-52}$ and its mutants ($D^{21} \rightarrow$ P and $D^{21} \rightarrow$ A) were transiently transfected into Jurkat cells together with a reporter plasmid in which the production of secreted alkaline phosphatase (SEAP) is under control of an IL-2 promoter carrying five GAL4-binding sites. Gel mobility-shift analyses of the cell lysates also were performed to assess the expression levels of the mutant proteins. Lane 2 shows a control with lysate of the cells transfected only with the reporter plasmid. In lane 6, an excess of unlabeled probe was used as competitor. The position of the protein–DNA complex is indicated by an arrowhead.

The crystal structure of the complex between $p53_{15-29}$ and MDM2 has identified Phe^{19}, Leu^{22}, Trp^{23}, and Leu^{26} of p53 as critical residues for the interaction with MDM2 (11). Leu^{26} of p53 lies outside the FXXΦΦ motif. Among p53, p65, and VP16, only p53 has a Trp at the end of the FXXΦΦ motif (Trp^{23}, Fig. 1*A*). We therefore reasoned that these two residues, Leu^{26} and Trp^{23}, might be responsible for the discrimination. To assess this possibility, mutants of the p53 activation domain were constructed and analyzed for the ability to bind TAF_{1-140} and $MDM2_{3-109}$ (Fig. 5*B*). Substitution of Trp^{23} with Leu, which resulted in retention of a FXXΦΦ sequence, greatly decreased MDM2 binding only and had no effect on TAF binding. Removal of Leu^{26} significantly reduced MDM2 binding but had no effect on TAF binding (Fig. 5*B*; compare $p53_{9-25}$ and $p53_{9-26}$). These data indicated that Trp^{23} and Leu^{26} are the primary elements that enable MDM2 to discriminate the $hTAF_{II}31$-binding site in p53 against those in VP16 and p65.

We next asked whether the *in vitro* specificity of MDM2 could be recapitulated in transiently transfected cells (Fig. 5*C*). The wild-type p53 activation domain fused to the GAL4 DNA-binding domain activated transcription of a reporter gene that was controlled by five GAL4 sites, and its transcriptional activation was greatly inhibited by MDM2 coexpression as reported previously (26). In contrast, MDM2 coexpression had little effects on transcriptional activation by the activation domains of VP16 and p65. The p53 mutant in which Trp^{23} was substituted by Leu still activated transcription, but its transcriptional activation was not influenced significantly by MDM2 coexpression. These results are in good agreement with the *in vitro* results and with the notion that MDM2 discriminates among FXXΦΦ motifs of $hTAF_{II}31$-dependent activators in the cells. This precise recognition permits MDM2 to specifically control the p53 protein in the presence of other $hTAF_{II}31$-dependent activators.

Although the Trp^{23}-Leu mutant bound TAF_{1-140} as tightly as the wild type in GST pull-down assays, its ability to activate transcription of the reporter gene in transfected cells was evidently less than that of the wild type. Presumably, the difference in affinity to TAF_{1-140} that was caused by the mutation is modest and undetectable in our GST pull-down assays. It is not clear how much of an affinity change is needed to clearly modulate the intensity of TAF_{1-140} bands on SDS/PAGE gels.

Discussion

Motifs in Transcriptional Activation Domains. Transcriptional activation domains share little sequence homology except a preponderance of particular amino acids (27). This low homology of

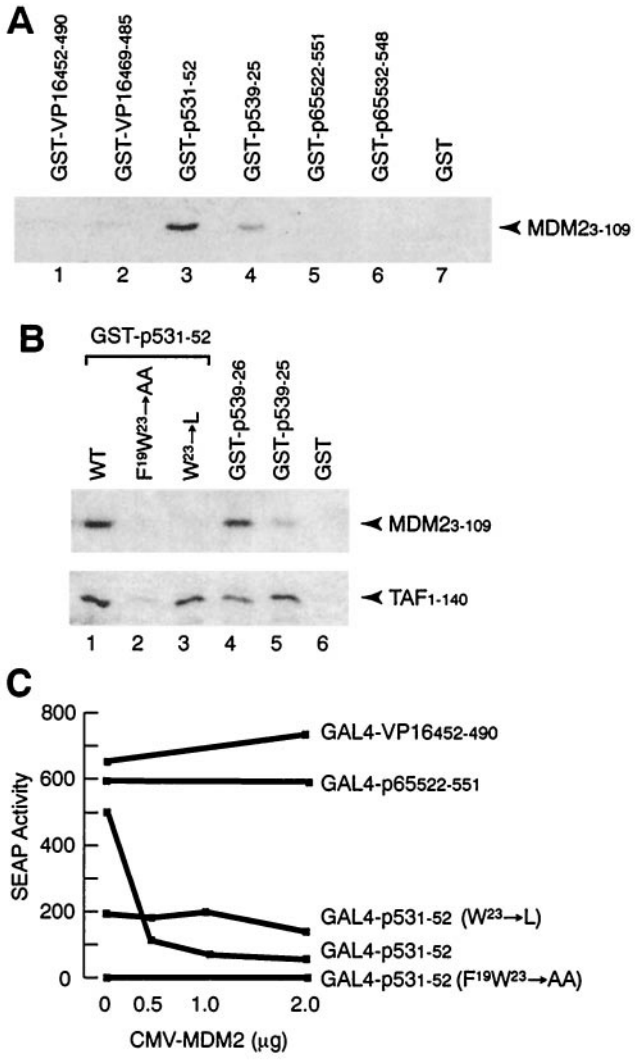

Fig. 5. MDM2 discriminates among FXXΦΦ motifs. (*A*) *In vitro* protein–protein interaction assays. Binding of GST-$p53_{1-52}$ (lane 3) to $MDM2_{3-109}$ is evident, and $MDM2_{3-109}$ is not retained on GST-$VP16_{452-490}$ (lane 1), GST-$VP16_{469-485}$ (lane 2), GST-$p65_{522-551}$ (lane 5), GST-$p65_{532-548}$ (lane 6), and GST (lane 7) resins. $MDM2_{3-109}$ binds to GST-$p53_{9-25}$ (lane 4) much more weakly than to GST-$p53_{1-52}$. (*B*) Effects of amino acid substitutions and deletion on the interaction of the p53 activation domain with $MDM2_{3-109}$ and TAF_{1-140} *in vitro*. The positions of $MDM2_{3-109}$ and TAF_{1-140} are indicated by arrowheads. (*C*) Effects of substitution of Trp^{23} on transcriptional activation in transfected cells and response to MDM2 coexpression. Increasing amounts of a plasmid encoding human MDM2 were transfected into Jurkat cells cotransfected with an expression plasmid of GAL4-$p53_{1-52}$ or its mutants and a reporter plasmid in which the production of secreted alkaline phosphatase (SEAP) is under control of an IL-2 promoter carrying five GAL4-binding sites.

activators, which presumably translates into a low affinity for their target proteins, has rendered activation domains elusive. Our results indicate that an FXXΦΦ sequence in the p53 activation domain is a short α-helical motif that is recognized by $hTAF_{II}31$. It is also shown that a short peptide from the p65 activation domain that encompasses an FXXΦΦ sequence binds $hTAF_{II}31$ and activates transcription. These results, together with those of the VP16 activation domain (18), strengthen the notion that the FXXΦΦ sequence is a general recognition element for $hTAF_{II}31$ and may be more generally a signature for acidic activators that interact with $hTAF_{II}31$.

Inspection of amino acid sequences of acidic activators identified potential FXXΦΦ motifs in a number of acidic activation domains including those of NFAT and BRCA1. Notably, a point mutation of the FXXΦΦ sequence of BRCA1 is associated with a preposition to breast and ovarian cancers and disrupts transcriptional activation by BRCA1 (28, 29). Moreover, the acidic activation domains of human GLI and yeast Adr1p recently have been suggested to carry potential FXXΦΦ motifs (30, 31). Although further work is needed to verify these putative motifs, it is likely that other acidic activators use FXXΦΦ motifs for interaction with $hTAF_{II}31$. Recently, four laboratories independently reported that functional inactivation of $yTAF_{II}17$, a yeast homolog of $hTAF_{II}31$, resulted in loss of transcription of many yeast genes (32–35). Genomewide expression analyses showed that the expression of approximately 67% of actively expressed yeast genes are as dependent on $yTAF_{II}17$ function as it is on core RNA polymerase itself (32, 35). These yeast studies suggest that homologues of $hTAF_{II}31$ have an important general role in eukaryotic transcription.

The interaction between a FXXΦΦ motif and $hTAF_{II}31$ shows similarities with the other recently described interactions between activators and their targets. The activation domain of cAMP-responsive element binding protein (CREB) binds to CREB binding protein (CBP) through a similar α-helical motif, YXXIL (36), and the interactions of coactivators SRC-1 and GRIP-1 with liganded nuclear receptors also are mediated by an α-helical LXXLL sequence (37–39). We favor the view that eukaryotic cells have evolved a transcriptional activation mechanism wherein protein–protein interactions within the preinitiation complex are mediated through such short amphipathic helical motifs that resemble each other. This may be a strategy for building dynamic and flexible transcriptional regulatory complexes that are required for specific and steep responses. Because it is now evident that TAFs are not the sole targets for activation domains (40), the FXXΦΦ motif must be just one of many interaction motifs in activation domains. Further identification of these motifs should be helpful for the full understanding of transcriptional activation domains and the dissection of complicated transcriptional regulation.

Insights into Regulation of the p53 Activation Domain. p53 activates transcription of the *mdm2* gene whereas its protein product MDM2 suppresses p53 activity (1). This creates an autoregulatory feedback loop in which both the activity of p53 and the expression of MDM2 are coregulated. Our results suggest that MDM2 inhibits p53 function by tightly masking the FXXΦΦ sequence of p53, which otherwise binds $hTAF_{II}31$ and activates transcription. Whereas the FXXΦΦ motifs in p65 and VP16 have no detectable affinity to MDM2, all three core domains containing FXXΦΦ motifs bind equally well to TAF_{1-140}. This promiscuity in binding to TAF_{1-140} but discrimination in binding to MDM2 enables all of the core domains to activate transcription yet only p53 to be inhibited by MDM2, all through interactions near a common peptide segment. Substitution of Trp^{23} with Leu in the p53 activation domain, which retains the FXXΦΦ sequence, abolished only MDM2 binding and had no effect on TAF binding, indicating that Trp^{23} is a major determinant for differential recognition by MDM2. It may be possible to develop indole-based small molecules that inhibit MDM2 but not $hTAF_{II}31$.

It has been reported that p300/CBP proteins interact with the p53 activation domain and potentiate the transcriptional activity of p53 (5–7). The p300/CBP interaction region appears to overlap with those of $hTAF_{II}31$ and MDM2, because a double point mutation of Leu^{22} and Trp^{23} abolishes binding with CBP (5). The involvement of the FXXΦΦ sequence of p53 in these multiple interactions suggests competitive binding of $hTAF_{II}31$, p300/CBP, and MDM2 to tetrameric p53. This situation has been complicated by the recent finding that $hTAF_{II}31$ is present

in the p300/CBP-associated factor (PCAF)-containing complex (41). Because PCAF interacts with p300/CBP, PCAF can be recruited to the promoter by binding to either $hTAF_{II}31$ or p300/CBP. PCAF is a histone acetyltransferase that plays a role in regulation of transcription, cell cycle progression, and differentiation. Recruitment of this important acetylase to p53-responsive promoters may be ensured by binding of the p53 activation domain to $hTAF_{II}31$ and p300/CBP.

The p53 activation domain is also regulated by DNA-dependent protein kinase (DNA-PK) and ATM kinase, which phosphorylate Ser^{15} of p53 in response to DNA damage (14, 15, 17). Ser^{15} of p53 is located four residues N-terminal to the FXXΦΦ motif, and the phosphorylation indeed disrupts the interaction with MDM2 (16). Interestingly, the ability of p53 to activate transcription is not affected by phosphorylation at Ser^{15} (16), suggesting that the phosphorylation at Ser^{15} does not interfere with the interactions with TAFs and p300/CBP (42). Although the association sites of $hTAF_{II}31$, p300/CBP, and MDM2 are centered around the FXXΦΦ motif, it seems clear that all these partially use distinct interaction modes for this α-helical module.

The FXXΦΦ sequence and its vicinity in the p53 activation domain functions as a small control unit integrating protein–protein interactions and posttranslational modification. Such a complex interplay of posttranslational modification and multiple protein–protein interactions offers a mechanism for dynamic control of responses.

We thank Drs. Arnold J. Levine, Hua Lu, Origène Nyanguile, James Falvo, and Brian Dynlacht for providing plasmid constructs and Yongmun Choi for technical assistance. This work was supported in part by a grant from the Hoffmann-La Roche Institute of Chemistry and Medicine, a National Science Foundation Presidential Young Investigator Award (G.L.V.), and the Leukemia Society of America (M.U.). The NMR spectrometer used in this work was purchased with funding from the National Science Foundation.

1. Levine, A. J. (1997) *Cell* **88,** 323–331.
2. Lu, H. & Levine, A. J. (1995) *Proc. Natl. Acad. Sci. USA* **92,** 5154–5158.
3. Thut, C. J., Chen, J. L., Klemm, R. & Tjian, R. (1995) *Science* **267,** 100–104.
4. Gu, W. & Roeder, R. G. (1997) *Cell* **90,** 595–606.
5. Gu, W., Shi, X. L. & Roeder, R. G. (1997) *Nature (London)* **387,** 819–823.
6. Avantaggiati, M. L., Ogryzko, V., Gardner, K., Giordano, A., Levine, A. S. & Kelly, K. (1997) *Cell* **89,** 1175–1184.
7. Lill, N. L., Grossman, S. R., Ginsberg, D., DeCaprio, J. & Livingston, D. M. (1997) *Nature (London)* **387,** 823–827.
8. Prives, C. (1998) *Cell* **95,** 5–8.
9. Jones, S. N., Roe, A. E., Donehower, L. A. & Bradley, A. (1995) *Nature (London)* **378,** 206–208.
10. Yew, P. R. & Berk, A. J. (1992) *Nature (London)* **357,** 82–85.
11. Kussie, P. H., Gorina, S., Marechal, V., Elenbaas, B., Moreau, J., Levine, A. J. & Pavletich, N. P. (1996) *Science* **274,** 948–953.
12. Haupt, Y., Maya, R., Kazaz, A. & Oren, M. (1997) *Nature (London)* **387,** 296–299.
13. Kubbutat, M. H., Jones, S. N. & Vousden, K. H. (1997) *Nature (London)* **387,** 299–303.
14. Canman, C. E., Lim, D. S., Cimprich, K. A., Taya, Y., Tamai, K., Sakaguchi, K., Appella, E., Kastan, M. B. & Siliciano, J. D. (1998) *Science* **281,** 1677–1679.
15. Banin, S., Moyal, L., Shieh, S., Taya, Y., Anderson, C. W., Chessa, L., Smorodinsky, N. I., Prives, C., Reiss, Y., Shiloh, Y., *et al.* (1998) *Science* **281,** 1674–1677.
16. Shieh, S. Y., Ikeda, M., Taya, Y. & Prives, C. (1997) *Cell* **91,** 325–334.
17. Woo, R. A., McLure, K. G., Lees-Miller, S. P., Rancourt, D. E. & Lee, P. W. (1998) *Nature (London)* **394,** 700–704.
18. Uesugi, M., Nyanguile, O., Lu, H., Levine, A. J. & Verdine, G. L. (1997) *Science* **277,** 1310–1313.
19. Nyanguile, O., Uesugi, M., Austin, D. J. & Verdine, G. L. (1997) *Proc. Natl. Acad. Sci. USA* **94,** 13402–13406.
20. Wu, Y., Reece, R. J. & Ptashne, M. (1996) *EMBO J.* **15,** 3951–3963.
21. Burley, S. K. & Roeder, R. G. (1996) *Annu. Rev. Biochem.* **65,** 769–799.
22. Campbell, A. P. & Sykes, B. D. (1993) *Annu. Rev. Biophys. Biomol. Struct.* **22,** 99–122.
23. Botuyan, M. V., Momand, J. & Chen, Y. (1997) *Fold Des.* **2,** 331–342.
24. Lin, J., Chen, J., Elenbaas, B. & Levine, A. J. (1994) *Genes Dev.* **8,** 1235–1246.
25. Chang, J., Kim, D. H., Lee, S. W., Choi, K. Y. & Sung, Y. C. (1995) *J. Biol. Chem.* **270,** 25014–25019.
26. Momand, J., Zambetti, G. P., Olson, D. C., George, D. & Levine, A. J. (1992) *Cell* **69,** 1237–1245.
27. Triezenberg, S. J. (1995) *Curr. Opin. Genet. Dev.* **5,** 190–196.
28. Monteiro, A. N., August, A. & Hanafusa, H. (1996) *Proc. Natl. Acad. Sci. USA* **93,** 13595–13599.
29. Chapman, M. S. & Verma, I. M. (1996) *Nature (London)* **382,** 678–679.
30. Yoon, J. W., Liu, C. Z., Yang, J. T., Swart, R., Iannaccone, P. & Walterhouse, D. (1998) *J. Biol. Chem.* **273,** 3496–3501.
31. Young, E. T., Saario, J., Kacherovsky, N., Chao, A., Sloan, J. S. & Dombek, K. M. (1998) *J. Biol. Chem.* **273,** 32080–32087.
32. Holstege, F. C., Jennings, E. G., Wyrick, J. J., Lee, T. I., Hengartner, C. J., Green, M. R., Golub, T. R., Lander, E. S. & Young, R. A. (1998) *Cell* **95,** 717–728.
33. Moqtaderi, Z., Keaveney, M. & Struhl, K. (1998) *Mol. Cell* **2,** 675–682.
34. Michel, B., Komarnitsky, P. & Buratowski, S. (1998) *Mol. Cell* **2,** 663–673.
35. Apone, L. M., Virbasius, C. A., Holstege, F. C., Wang, J., Young, R. A. & Green, M. R. (1998) *Mol. Cell* **2,** 653–661.
36. Radhakrishnan, I., Perez-Alvarado, G. C., Parker, D., Dyson, H. J., Montminy, M. R. & Wright, P. E. (1997) *Cell* **91,** 741–752.
37. Nolte, R. T., Wisely, G. B., Westin, S., Cobb, J. E., Lambert, M. H., Kurokawa, R., Rosenfeld, M. G., Willson, T. M., Glass, C. K. & Milburn, M. V. (1998) *Nature (London)* **395,** 137–143.
38. Shiau, A. K., Barstad, D., Loria, P. M., Cheng, L., Kushner, P. J., Agard, D. A. & Greene, G. L. (1998) *Cell* **95,** 927–937.
39. Darimont, B. D., Wagner, R. L., Apriletti, J. W., Stallcup, M. R., Kushner, P. J., Baxter, J. D., Fletterick, R. J. & Yamamoto, K. R. (1998) *Genes Dev.* **12,** 3343–3356.
40. Tansey, W. P. & Herr, W. (1997) *Cell* **88,** 729–732.
41. Ogryzko, V. V., Kotani, T., Zhang, X., Schlitz, R. L., Howard, T., Yang, X. J., Howard, B. H., Qin, J. & Nakatani, Y. (1998) *Cell* **94,** 35–44.
42. Lambert, P. F., Kashanchi, F., Radonovich, M. F., Shiekhattar, R. & Brady, J. N. (1998) *J. Biol. Chem.* **273,** 33048–33053.